Controlling Two-Step Multimode Switching of Dihydroazulene Photoswitches

ARTICLE *in* CHEMISTRY - A EUROPEAN JOURNAL · JANUARY 2015

Impact Factor: 5.73 · DOI: 10.1002/chem.201405457 · Source: PubMed

ChemPubSoc Europe

DOI: 10.1002/chem.201405457

CHEMISTRY A European Journal Full Paper

Photoswitches | *Hot Paper*

Controlling Two-Step Multimode Switching of Dihydroazulene Photoswitches

Anne U. Petersen, Søren L. Broman, Stine T. Olsen, Anne S. Hansen, Lin Du, Anders Kadziola, Thorsten Hansen, Henrik G. Kjaergaard, Kurt V. Mikkelsen, and Mogens Brøndsted Nielsen*[a]

Abstract: We present the synthesis and switching studies of systems with two photochromic dihydroazulene (DHA) units connected by a phenylene bridge at either *para* or *meta* positions, which correspond to a linear or cross-conjugated pathway between the photochromes. According to UV/Vis absorption and NMR spectroscopic measurements, the *meta*-phenylene-bridged DHA–DHA exhibited sequential light-induced ring openings of the two DHA units to their corresponding vinylheptafulvenes (VHFs). Initially, the VHF–DHA species was generated, and, ultimately, after continued irradiation, the VHF–VHF species. Studies in different solvents and quantum chemical calculations indicate that the excitation of DHA–VHF is no longer a local DHA excitation but a charge-transfer transition that involves the neighboring VHF unit. For the linearly conjugated *para*-phenylene-bridged dimer, electronic communication between the two units is so efficient that the photoactivity is reduced for both the DHA–DHA and DHA–VHF species, and DHA–DHA, DHA–VHF, and VHF–VHF were all present during irradiation. In all, by changing the bridging unit, we can control the degree of stepwise photoswitching.

Introduction

A molecular switch is a system that can interconvert reversibly between at least two different states when a stimulus is introduced.[1] For photoswitches, the stimulus is light.[2] Suitably designed photoswitches have generated interest as components for molecular electronics devices, information storage, molecular machines and sensors, control of chemical reactions, and as units to control folding and assembly of proteins and other biomolecules.[3] Thoroughly investigated examples of photoswitches are, in particular, those of *cis*/*trans*-azobenzene and dithienylethene (DTE)/dihydrothienobenzothiophene (DHB),[3] which can interconvert between their two isomers by irradiation, thus reaching a photostationary state that depends on the degree of overlap between the absorption spectra and that sometimes presents a drawback for these systems.

The dihydroazulene (DHA)/vinylheptafulvene (VHF) couple presents a system that is photoactive in one direction and thermally active in the other.[4] Upon irradiation with light ($\approx$ 350 nm), DHA undergoes a ten π-electron retro-electrocyclization to form the *meta*-stable VHF, which in turn can undergo a thermally induced ring closure back to DHA (Scheme 1). A major advantage of the DHA/VHF system is that, because only the DHA is photochromic and the VHF is long-lived ($t_{1/2}$ up to 1600 min in CH_3CN at 25 °C for certain derivatives), a complete conversion between the two states is possible.[5] This reversible switching has rendered DHA a particularly interesting candidate not only for molecular electronics[6] and molecular sensors,[7] but possibly also for the development of solar-energy storage devices, which harvest and store sunlight and release it again as heat when needed.[8]

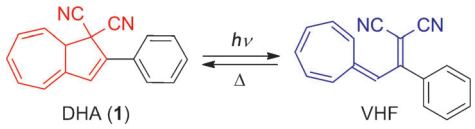

Scheme 1. DHA–VHF isomerizations: Light-induced ring opening of DHA to VHF and thermally induced ring closure of VHF to DHA.

To enable the use of DHA/VHF in advanced devices, the switching properties of the system need to be controlled. Fine-tuning of the rate of ring closure (VHF→DHA) has been accomplished by substitution with either electron-withdrawing and/or -donating groups with kinetics behavior that satisfies Hammett correlations,[9] and it has also been shown that having a strong electron acceptor such as a buckminsterfullerene (C_{60}) covalently attached to DHA quenches the light-induced ring opening.[10] Also, by reversible oxidation of a covalently attached ferrocene or tetrathiafulvalene unit,[11] or by protonation of an aniline substituent[9a,b] the photochromism of the DHA/VHF couple can be controlled. Along this line, mol-

[a] *A. U. Petersen, Dr. S. L. Broman, S. T. Olsen, A. S. Hansen, Prof. Dr. L. Du, Prof. Dr. A. Kadziola, Prof. Dr. T. Hansen, Prof. Dr. H. G. Kjaergaard, Prof. Dr. K. V. Mikkelsen, Prof. Dr. M. Brøndsted Nielsen*
Department of Chemistry and Center for Exploitation of Solar Energy
University of Copenhagen
Universitetsparken 5, 2100 Copenhagen (Denmark)
E-mail: mbn@kiku.dk

Supporting information for this article is available on the WWW under http://dx.doi.org/10.1002/chem.201405457.

ecules with two photochromic units have attracted interest as multimode switches. For example, for a dimeric DTE compound, it was shown that one DTE could be partly converted into DHB upon irradiation before this conversion occurred for the other DTE unit.[12] In two other examples, only one of the DTE units was photochromic, which showed the significance of the bridging unit between the DTEs.[13] DHA and DTE have also been combined in one example.[14] By using light/heat stimuli, conversion between three states of this system was accomplished. Unfortunately, DHA and the DTE have similar excitation wavelengths, which prevented us from addressing only one unit in a controlled manner. In another example, the DHA/VHF system was attached to a tetraethynylethene (TEE) that incorporated an aniline unit.[15] Here, a combination of light-induced *cis–trans* isomerization of the TEE and ring opening/closure of DHA/VHF together with acid/base control of the aniline allowed for interconversion between six states of the system.

We became interested in investigating the possibility of controlled multimodal switching of DHA/VHF in molecules that contained two DHA units covalently linked together by a central benzene ring. We reasoned that any communication between the two units could depend on the positions of these on the benzene ring (*meta* or *para*) and that the photoactivity of one DHA could depend on whether its neighboring unit had already been converted to VHF. Here we present the synthesis and properties, on the basis of both experimental and computational studies, of such multichromophore systems that connect two DHA/VHF units through either a *para*-phenylene (**2**) or a *meta*-phenylene (**3**) bridge (Figure 1). Indeed, these different configurations turn out to have a detrimental influence on the extent to which the two DHAs communicate and whether one DHA unit can be addressed selectively.

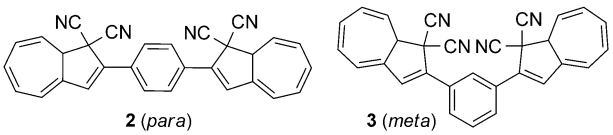

Figure 1. Dimeric DHA photoswitches with *para*- (linearly conjugated) and *meta*- (cross-conjugated) phenylene spacers.

Results and Discussion

Synthesis and X-ray crystallography

The *para*-phenylene-bridged DHA–DHA **2** was synthesized according to an analogous procedure for making the monomeric DHA **1**.[5e,15,16] First, a Knoevenagel condensation between 1,4-diacetylbenzene and malononitrile in a buffer solution of hexamethyldisilazane (HMDS) and acetic acid (AcOH) at 70 °C gave the known[17] crotononitrile **4** in a yield of 98% (Scheme 2). In the next step, this compound was initially treated with tropylium tetrafluoroborate (2 equiv) at −78 °C in CH_2Cl_2 under slow addition of Et_3N (not shown in Scheme 2), which gave the alkylated intermediate **5** as the major product (>90%). The crude alkylated intermediate was heated to reflux with tritylium tetrafluoroborate (2 equiv) for two hours in 1,2-dichloroethane (DCE). After being cooled to 0 °C and diluted with toluene, Et_3N was added, thereby furnishing the *para*-substituted VHF–VHF **6**, which was then heated to finally provide the *para*-substituted DHA–DHA **2**. This compound was isolated almost pure in a yield of 34% (as a mixture of diastereoisomers) after column chromatography; an analytically pure sample could be obtained from recrystallization from CH_3CN. When too much tropylium tetrafluoroborate was added in the initial step, a complex mixture of photochromic molecules was obtained (see the Supporting Information). In an attempt to ease the purification, the alkylation was carried out in a different manner, as outlined in Scheme 2. Compound **4** was deprotonated twice using 2.2 equivalents of lithium bis(trimethylsilyl)-amide (LiHMDS) at −78 °C to form the dicarbanion, and subsequently tropylium tetrafluoroborate was added to give **5** as the major product (>90%). The following step was carried out as described above, which gave the final product **2** in an overall yield of 87% with minor impurities, and after recrystallization in a yield of 21%. The identity of the final DHA dimer **2** was ultimately confirmed by X-ray crystallographic analysis (Figure 2). The two DHA units are perfectly coplanar, whereas the *para*-phenylene between them is twisted by 27° relative to this plane.

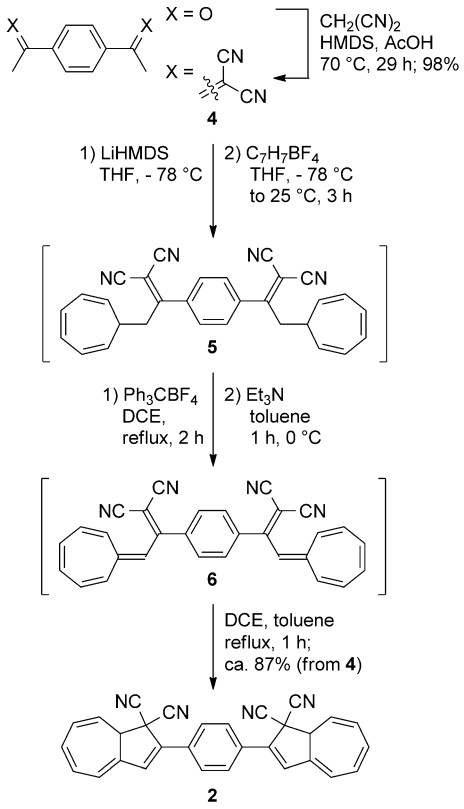

Scheme 2. Synthesis of the *para*-phenylene-bridged dimeric DHA compound.

To optimize the yield, a different route to the *para*-phenylene-bridged DHA–DHA **2** was attempted (Scheme 3). At this

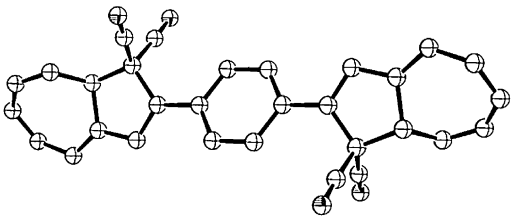

Figure 2. Molecular structure of DHA–DHA **2** (*para*; crystals grown from CH_3CN) with displacement ellipsoids at 50% probability. For clarity, hydrogen atoms are not shown.

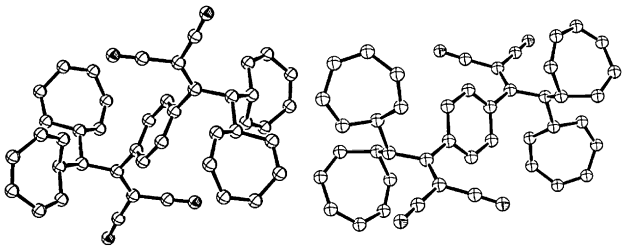

Figure 3. Molecular structures of **7** with displacement ellipsoids at 50% probability based on two polymorphic crystals grown from chloroform/heptane. Left: Structure obtained from red crystal (half of a unit cell is shown). Right: Structure obtained from yellow crystal. For clarity, hydrogen atoms are not shown.

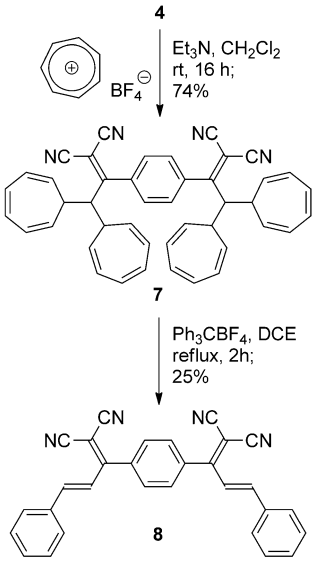

Scheme 3. Attempted synthesis of **2**, which instead gave a product resulting from ring contraction of two cycloheptatrienes.

point two cycloheptatriene units were incorporated at each side of the crotononitrile **4** because it has previously been shown that tropylium can act as a leaving group in a subsequent elimination step.[18] Treatment with tropylium tetrafluoroborate (5 equiv) gave product **7** in a yield of 74%. A subsequent oxidation of **7** was carried out with tritylium tetrafluoroborate in DCE under reflux conditions for 2 h, which, however, only facilitated a ring contraction on both sides of the phenylene ring. Thus product **8** was isolated in 25% yield; such ring contractions are known to occur for cycloheptatrienes with a leaving group at the substituent on C-9 of the cycloheptatriene.[19] Performing the reaction at room temperature in DCE or changing the oxidizing agent to 1,2-dichloro-3,4-dicyanoquinone (DDQ) gave rise to a complex mixture of photochromic compounds that contained only trace amounts of **2**, from which we could isolate (in approximately 17% yield) the mixed version of **2** and **8** with one DHA unit and one phenylallylidenemalononitrile unit (see the Supporting Information).

Recrystallization of **7** gave a mixture of yellow and red crystals, which were both subjected to X-ray crystallographic analysis (Figure 3). Different packing of the molecules in the two crystals might account for the different colors.

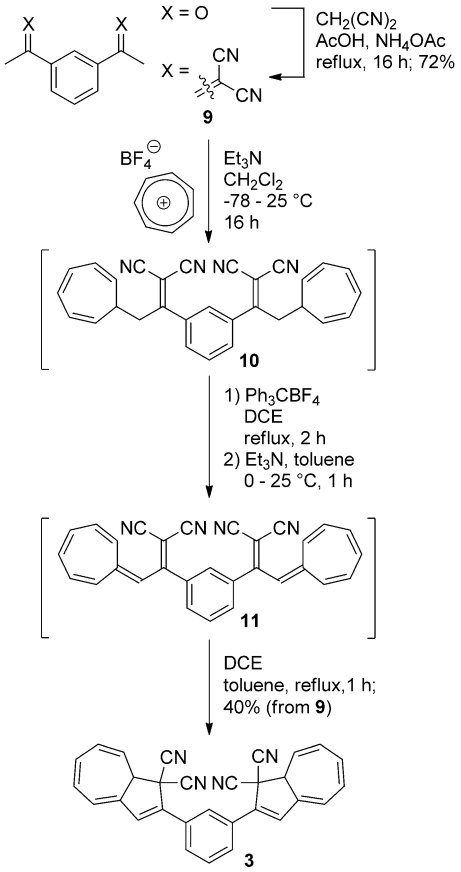

Scheme 4. Synthesis of *meta*-phenylene-bridged dimeric DHA compound.

To make the *meta*-phenylene-bridged DHA–DHA **3**, we returned to the original strategy in which only one cycloheptatriene is incorporated at each end of the molecule. A three-step procedure is shown in Scheme 4. First, a Knoevenagel condensation between 1,3-diacetylbenzene and malononitrile in toluene heated to reflux by using AcOH/NH_4OAc as buffer gave product **9** in 53% yield after fractional recrystallization. For this step, the often preferred AcOH/HMDS buffer for condensation of methylarylketones with electron-withdrawing groups only gave the desired compound **9** in a trace amount. Next, **9** was treated with tropylium tetrafluoroborate in CH_2Cl_2

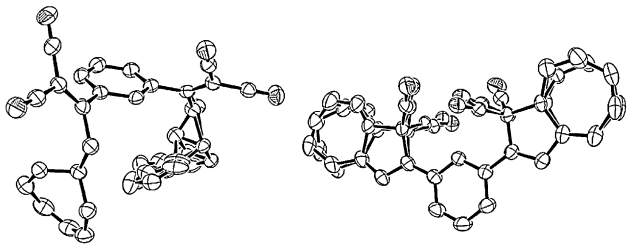

Figure 4. Molecular structures of (left) **10** (crystals grown from CH_2Cl_2/heptanes) and (right) DHA–DHA **3** (*meta*; crystals grown from CH_2Cl_2/heptanes) with displacement ellipsoids at 50% probability. For clarity, hydrogen atoms are not shown.

at −78 °C followed by slow addition of Et_3N until the starting material was fully consumed (approximately 2 equiv). From the mixture of alkylated intermediates, the major product **10** could again be isolated by recrystallization and its structure was confirmed by X-ray crystallography as shown in Figure 4 (left). The crude mixture was then treated with tritylium tetrafluoroborate in DCE heated at reflux for two hours followed by Et_3N at 0 °C in toluene, which gave VHF–VHF **11** as judged by thin-layer chromatographic analysis (a red spot that turned yellow upon heating). After heating to reflux for one hour, VHF–VHF **11** was converted into DHA–DHA **3**, which was isolated by dry column vacuum chromatography as a mixture of diastereoisomers and in an overall yield of 40% from **9**. The structure of DHA–DHA **3** was ultimately confirmed by X-ray crystallography (showing some disorder) as depicted in Figure 4 (right). Interestingly, whereas the conformation of DHA–DHA **3** has the two DHA units oriented in the same direction in the crystal, DHA–DHA **2** has them oriented in opposite directions.

UV/Vis absorption spectroscopy and switching studies

The two dimeric DHA compounds **2** and **3** are both photochromic in CH_3CN, CH_2Cl_2, PhMe, and cyclohexane (C_6H_{12}), but with significantly different photoactivities (see below). By irradiation with light at their absorption maxima (which requires more intense light for **2**), as listed in Table 1, a new band at around 460 nm appeared that was characteristic of VHF formation, whereas the characteristic DHA absorption band disappeared. Absorption spectra are shown in Figure 5a and b. Likewise the VHFs undergo thermally induced ring closures back to the DHAs. After conversion of DHA–DHA **3** to VHF–VHF **11**, the decay of the VHF absorption band (VHF–VHF/DHA–VHF) was followed in time, thereby providing the rate constants listed in Table 2. Interestingly, the rate of ring closure of VHF–VHF **11** to **3** through the intermediate DHA–VHF changed during the back-reaction as two exponential functions were needed to fit the decay in VHF absorbance. Thus, the first ring closure was found to have a longer half-life than the second ring closure. This effect is largest in CH_2Cl_2, in which the rate constants are 2.0×10^{-5} and 3.3×10^{-5} s^{-1} for the first and second ring closure, respectively (Table 2); these correspond to half-lives of 572 and 346 min. Notably, the DHA and VHF absorption maxima in the isomers of **3** depend on the identity of the neighboring unit and hence shift slightly in DHA–DHA, DHA–VHF, and VHF–VHF.

The nature of the bridge had a significant influence on the light-induced ring-opening reactions. Thus, the *para*-phenylene-bridged DHA–DHA **2** was quite reluctant to undergo ring opening and could not be fully converted to the VHF–VHF **6** with the lamp successfully used to convert DHA–DHA **3** to VHF–VHF **11**. Instead, we had to use a more intense lamp with a broader wavelength spectrum and higher radiation energy

Table 1. Absorption maxima for **1**, **2**, and **3**.

	Solvent	$\lambda_{max}^{DHA-DHA}$ [nm]	$\lambda_{max}^{DHA-VHF}$ [nm] (DHA part)	$\lambda_{max}^{DHA-VHF}$ [nm] (VHF part)	$\lambda_{max}^{VHF-VHF[a]}$ [nm]
1	CH_3CN	355	–	470	–
	PhMe	360	–	464	–
	C_6H_{12}	354	–	446	–
2 (*para*)	CH_3CN	408	[b]	[b]	466 (**6**)
	PhMe	416	[b]	[b]	467 (**6**)
	C_6H_{12}	408	[b]	[b]	450 (**6**)
3 (*meta*)	CH_3CN	365	360	476	466 (**11**)
	CH_2Cl_2	367	361	478	469 (**11**)
	PhMe	369	–	473	466 (**11**)
	C_6H_{12}	363	353	454	449 (**11**)

[a] Compound number of the VHF–VHF is provided in brackets. [b] Absorption maxima are not provided owing to the overlapping bands of DHA–DHA, DHA–VHF, and VHF–VHF (but a spectrum of the mixture is shown in Figure 5a).

Table 2. Characteristics of DHA→VHF conversions and rate of back-reaction (VHF→DHA at temperature *T*) for DHAs **1** and **3**.

	Solvent	τ_1/τ_2[a]	*T* [°C]	$k_{VHF\rightarrow DHA}$ [10^{-5} s^{-1}]	$t_{1/2\,VHF\rightarrow DHA}$ [min]
1	CH_3CN	–	25	5.36	216
	CH_2Cl_2	–	25	2.12	545
	PhMe	–	25	0.78	1474
	C_6H_{12}	–	25	0.50	2333
	C_6H_{12}	–	70	64.3	18.0
3 (*meta*)	CH_3CN	29	25	7.2→8.2[b]	160→140[b]
	CH_2Cl_2	34	25	2.0→3.3[b]	572→346[b]
	PhMe	26	–	–	–
	C_6H_{12}	14	70	53→62[b]	21→19[b]

[a] Ratio between time constants (τ_1/τ_2) determined from a double-exponential fit of the VHF absorbance increase over time, corresponding to the stepwise conversions of DHA–DHA to DHA–VHF and DHA–VHF to VHF–VHF (see Scheme 5). [b] The rate constant gradually increased during the experiment.

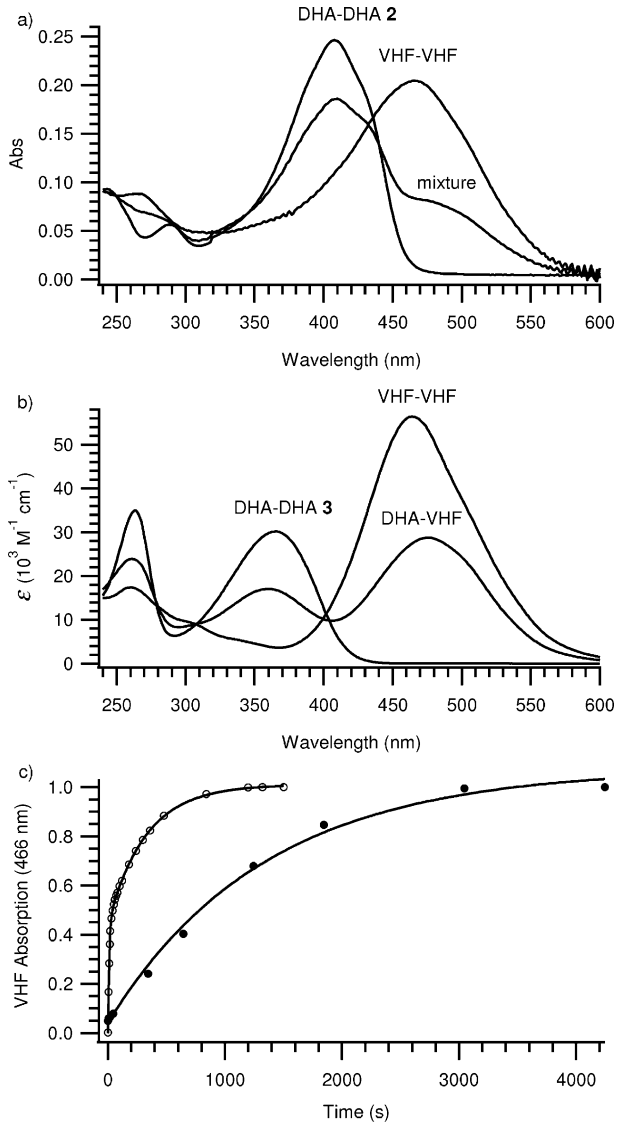

Figure 5. a) UV/Vis absorption spectra in CH_3CN of DHA–DHA **2** (*para*; concentration: 5.89×10^{-6} M), its corresponding VHF–VHF (**6**), and a mixture of the DHA–DHA, DHA–VHF, and VHF–VHF. b) UV/Vis absorption spectra in CH_3CN of DHA–DHA **3** (*meta*) and its corresponding DHA–VHF and VHF–VHF (**11**). c) VHF absorbance in CH_3CN at absorption maximum (normalized to unity for the final species) as a function of time of light irradiation: DHA–DHA→DHA–VHF→VHF–VHF for **3** (open circles) and **2** (filled circles). Irradiation of **2** was performed using a light source (four lamps) with a broad radiation around 368 nm, whereas irradiation of **3** was carried out using a less intense 150 W xenon arc lamp equipped with a monochromator set at a wavelength of 365 nm. Thus, the timescales for DHA-to-VHF conversions for the two compounds cannot be directly compared in this figure, but it is clear that both ring openings of DHA–DHA **3** occur faster than those of DHA–DHA **2** as less intense light is used for **3**.

to achieve full conversion to the VHF–VHF (for details on the homebuilt lamp setup, see the Supporting Information). We explain this reduced quantum yield of ring opening of **2** by a change in the chromophore part by the linearly conjugated bridge in line with the redshifted absorption maximum (408 nm in CH_3CN) relative to that of DHA **1** (355 nm in CH_3CN), which is also supported by a computational study (see below). Figure 5c shows the increase in the VHF absorbance (normalized to unity for the final VHF–VHF species) during irradiation. The data points for compound **2** could be fitted by one exponential function, which indicates that the two DHAs are opened nonselectively (i.e., with similar quantum yields, which are very small). We also subjected a sample to NMR spectroscopic studies between irradiations. The spectra show that all three species—DHA–DHA, DHA–VHF, and VHF–VHF—are present; this is most clearly seen from the different resonances of the phenylene protons for the three species (Figure 6).

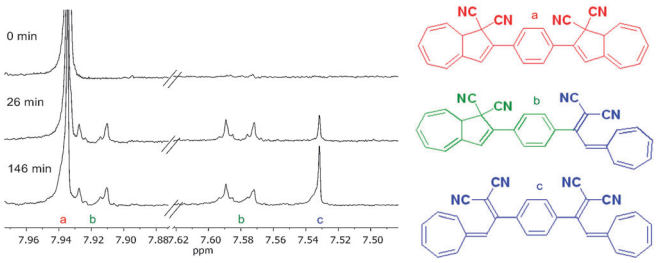

Figure 6. Part of the ^{1}H NMR spectrum (500 MHz, CD_3CN) of DHA–DHA **2** before and after exposure to light. The spectra show the phenylene resonances of the DHA–DHA, DHA–VHF, and VHF–VHF (which correspond to **6**) species, all present after some minutes of irradiation.

When placed in a *meta* arrangement (**3**), the two photochromic DHA units undergo stepwise ring openings according to Figure 5c and illustrated in Scheme 5. In CH_3CN, the first ring opening of **3** (DHA–DHA→DHA–VHF) proceeded with a high quantum yield ($\Phi_1 = 0.65$, estimated by comparison to parent DHA; see the Supporting Information) very similar to that of the parent DHA **1** ($\Phi = 0.55$). However, the second ring opening (DHA–VHF→VHF–VHF) is characterized by a much lower quantum yield. Figure 5c shows the change in the VHF absorp-

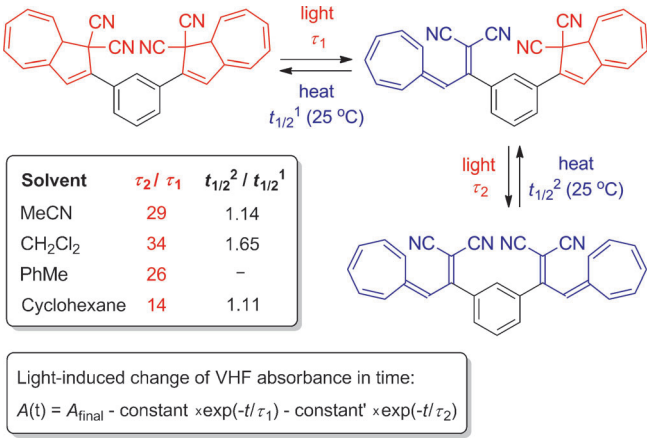

Scheme 5. Stepwise ring openings of the two DHAs in the *meta*-phenylene-bridged DHA–DHA **3** to VHF–VHF, which returns to DHA–DHA through DHA–VHF with two different half-lives. On account of the large difference in the two time constants, τ_1 and τ_2, obtained from the double-exponential fit, they are for simplicity assigned to each of the two consecutive ring-opening reactions in the scheme (for illustrative purposes only); this separation is only an approximation.

tion during irradiation; it is clearly visible that the first ring opening took place within the first 35 s of irradiation, after which the change in absorption slowed, and after another 1500 s of irradiation, the second DHA unit had been fully opened to VHF. By fitting the VHF absorption against time of irradiation with a double-exponential fit, the ratio between time constants was determined to be 29 (Scheme 5). In effect, one can almost selectively open one DHA unit without affecting the second. The sequential ring openings appear stepwise with isosbestic points in the UV/Vis absorption spectra, but as the isosbestic points are located at two different wavelengths (in CH_3CN at 404 and 399 nm, respectively), they will appear to move slightly during the two ring openings (see the Supporting Information). The sequential ring openings were also observed in CH_2Cl_2, toluene, and C_6H_{12}. Importantly, in polar solvents the sequential switching is more dominant than in non-polar solvents (see Table 2). Thus, the ratio between time constants is significantly reduced from 29 in acetonitrile to 14 in cyclohexane. This observation suggests that quenching of DHA photoactivity in DHA–VHF is related to a charge-transfer mechanism, which is supported by a computational study (see below). All photoswitching experiments were performed in non-deoxygenated solvents because it has previously been shown that such precautions do not significantly improve the stability of the DHA chromophore.[5c] In non-deoxygenated CH_3CN, a photodegradation of approximately 6.6% was observed for **3** after seven full light/heat cycles, whereas a value of 3.4% was obtained in deoxygenated CH_3CN (see the Supporting Information).

We also followed the initial DHA–DHA **3** to DHA–VHF conversion by means of NMR spectroscopy as shown in Figure 7. The evolution of the NMR spectra during irradiation confirms the stepwise ring opening (a longer irradiation time is needed owing to the larger concentration used in the NMR spectroscopic experiment relative to the UV/Vis experiment). As the DHA–DHA **2** could not be opened by the light source used to open both DHAs of DHA–DHA **3**, we can infer that the quantum yield must be even smaller than that of the DHA–VHF of **3**; a rough estimate indicates that the quantum yield must be below 1% for **2**.

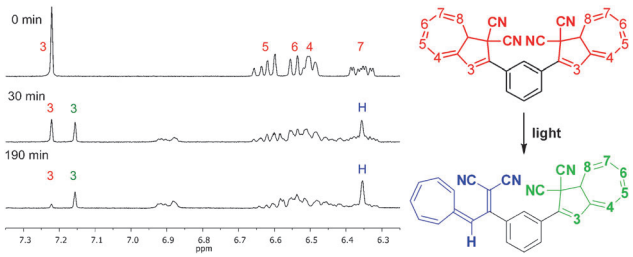

Figure 7. Part of the ^{1}H NMR spectrum (300 MHz, CD_3CN) of DHA–DHA **3** before and after exposure to light. The H3 resonance of DHA–DHA **3** disappears along with the appearance of the upfield-shifted DHA H3 resonance and VHF exocyclic fulvene CH resonance of DHA–VHF, whereas signals from VHF–VHF (which correspond to **11**) are not observed.

Computational study

To shed light on the origin of the reduced photoactivity of **2** and its DHA–VHF isomer and the sequential ring openings of **3**, we subjected the compounds to a detailed computational study. Optimization of the compounds was performed in Gaussian 09[20] using the polarizable continuum model (PCM) method and the CAM-B3LYP/cc-pVDZ level of theory. The optimized structures (with VHFs in *s-cis* conformations) were subjected to vertical excitation-energy calculations using the TD-CAM-B3LYP/cc-pVDZ method. To verify the method of DFT/CAM-B3LYP, CC2/cc-pVDZ excitation calculations were performed in TURBOMOLE[21] and are listed in Table 3. The gas-phase-calculated CC2 absorption maxima are in good agreement with the DFT/CAM-B3LYP-calculated ones for both the DHA–DHA and the DHA–VHF compounds in *meta* and *para* positions. DFT data for the DHA **1** are also included in Table 3 for comparison.

The influence of polar solvents (water and acetonitrile) was studied next. As expected, these media provided redshifted absorption maxima relative to the gas-phase values. Longest-wavelength absorption maxima at 386 and 359 nm were obtained for DHA–DHAs **2** and **3**, respectively, in CH_3CN, and similar values of 395 and 359 nm, respectively, in H_2O. These calculated values are in good agreement with the experimental absorption maxima of these DHA–DHA compounds (408 and

Table 3. Absorption maxima calculated using the PCM method and CAM-B3LYP/cc-pVDZ and CC2/cc-pVDZ levels of theory. Oscillator strengths are provided in brackets.

	Medium	λ_{max}^{DFT} [nm] DHA–DHA or DHA	λ_{max}^{DFT} [nm] DHA–VHF or VHF	λ_{max}^{CC2} [nm] DHA–DHA or DHA	λ_{max}^{CC2} [nm] DHA–VHF or VHF
1	vacuum	337 (0.44)	403 (0.03)	321 (0.53)	402 (0.33)
	H_2O	351 (0.54)	432 (0.67)		
	CH_3CN	351 (0.54)	432 (0.67)		
2 (*para*)	vacuum	384 (1.30)	363 (0.80), 401 (0.30), 414 (0.25)	366 (1.57)	428 (0.35) (VHF unit)
	H_2O	395 (1.47)	373 (0.85), 407 (0.05), 448 (0.72)		
	CH_3CN	386 (1.31)	373 (0.85), 407 (0.05), 448 (0.71)		
3 (*meta*)	vacuum	352 (0.79)	341 (0.43), 400 (0.36), 413 (0.22)	331 (0.94)	426 (0.28) (VHF unit)
	H_2O	359 (0.91)	350 (0.53), 406 (0.04), 444 (0.70)		
	CH_3CN	359 (0.92)	350 (0.53), 406 (0.04), 444 (0.70)		

365 nm in CH_3CN). Figure 8 shows the simulated spectra for DHA **1** and DHA–DHAs **2** and **3** in CH_3CN. The redshifted absorption maximum of **2** signals that the *p*-phenylene bridge has changed the chromophore significantly, which could explain the lower quantum yield of ring opening (the chromophore has less DHA character). The orbitals that correspond to the DHA excitations for **2** are shown in Figure 9 relative to those of DHA–VHF of **2** and those of DHA–DHA/DHA–VHF of **3**. All these plots are from the calculations with H_2O, in which differences between orbitals are most significant and hence most illustrative for a qualitative discussion. Both the HOMO and LUMO of **2** are significantly delocalized along the entire molecule with significant density on the central benzene ring; these two orbitals are the most important in describing the transition (molecular orbital coefficient of 0.43). The chromophore is accordingly significantly changed from being just a simple DHA, in accordance with its reluctance to undergo conversion to DHA–VHF. For the DHA–VHF form of **2**, the calculation provides a vertical electronic DHA transition at 373 nm. This excitation involves a transition from the HOMO−1 to the LUMO and LUMO+2, and as the LUMO is mainly situated at the VHF, this transition has significant charge-transfer character, which can account for the reluctance of this isomer of **2** as well to undergo DHA ring opening (no longer a local DHA excitation). For the DHA–DHA of **3**, the vertical electronic DHA transition is at 359 nm in both CH_3CN and H_2O, hence slightly redshifted relative to that calculated for **1** in these solvents (351 nm) and in agreement with experimental observations. For the DHA–VHF isomer of **3**, a vertical electronic "DHA transition" is calculated at 350 nm (hence slightly blueshifted relative to the DHA–DHA, also in agreement with experimental results). This excitation involves a transition from the HOMO−1 (located mainly at the DHA) to the LUMO+1 and LUMO+2 and only to a small extent to the LUMO (Figure 9). Both LUMO+1 and LUMO+2 are partly on the VHF, albeit not to the same extent as the LUMO, and the transition thus has charge-transfer character and is not a localized DHA excitation. It seems therefore very reasonable that the DHA–VHF of **3** undergoes less efficient ring opening to form VHF–VHF as observed experimentally, particularly in polar solvents.

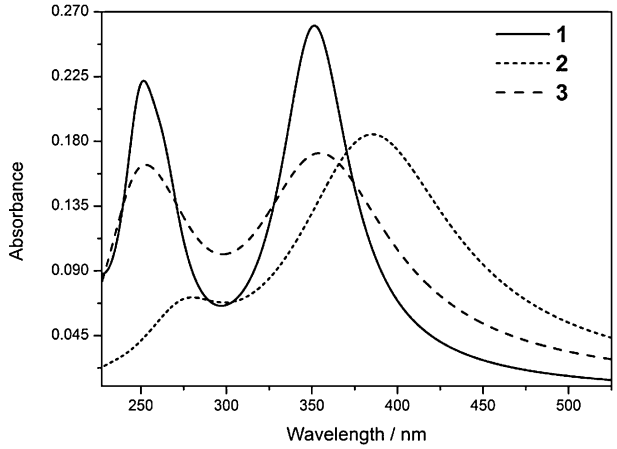

Figure 8. Calculated absorption spectra of DHA **1** and DHA–DHA isomers **2** (*para*) and **3** (*meta*) in CH_3CN using CAM-B3LYP/cc-pVDZ.

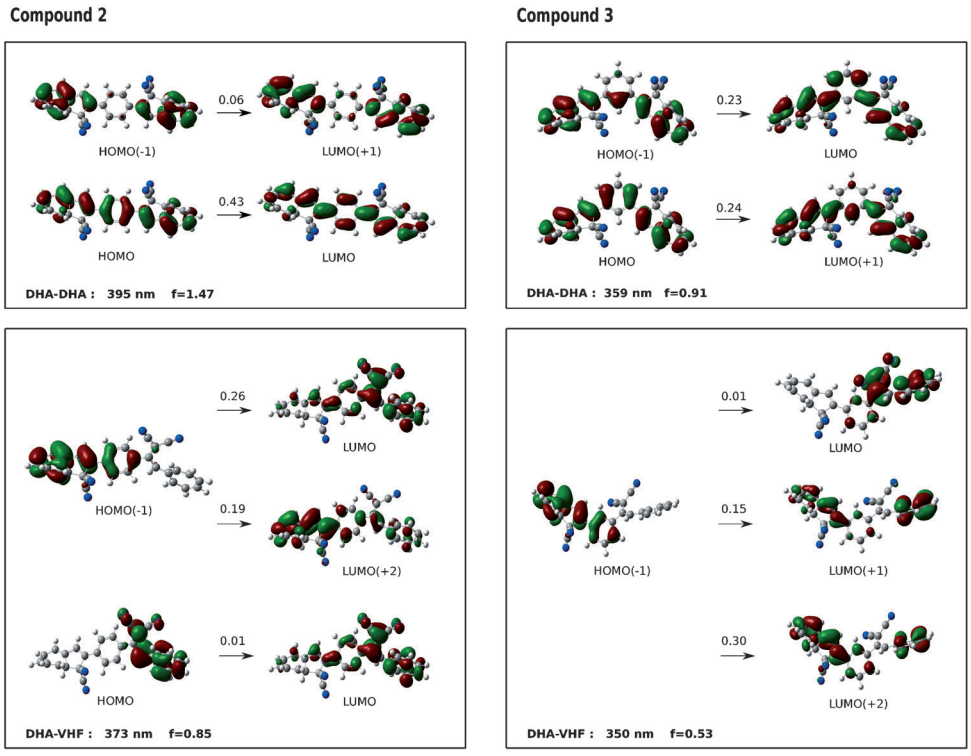

Figure 9. Orbitals corresponding to the "DHA excitations" for the DHA–DHA and DHA–VHF isomers of **2** and **3** in H_2O. The molecular orbital coefficient is shown above each arrow and the oscillator strength (*f*) of the overall transition is provided.

Conclusion

In conclusion, we have prepared a multimode photoswitch based on two DHA units separated by a *meta*-phenylene bridge (**3**) that is capable of sequential switching between three states (i.e., DHA–DHA, DHA–VHF, VHF–VHF) when using light as a stimulus. The sequential light-induced ring openings were explained by a significantly reduced photoactivity of the DHA when a neighboring VHF electron acceptor is present (DHA–VHF) as calculations show that the excitation has significant charge-transfer character instead of being a localized DHA excitation. For a *para*-phenylene-bridged DHA

dimer (**2**), we found that the DHA ring openings were strongly inhibited for the initial DHA–DHA species (which exhibited an even smaller photoactivity than that of the DHA–VHF of **3**). This bridging unit separates the two DHA units by a linearly conjugated pathway. The chromophore is hereby significantly altered and it was found to exhibit a redshifted absorption maximum relative to both a monomeric DHA and to the cross-conjugated *meta*-phenylene-bridged DHA dimer **3**. Future work will seek to investigate the influence of separating the two DHAs by other spacers and having more than two DHA units working in concert in related DHA oligomers. Further functionalization of the DHA dimers in the seven-membered rings by our previously developed[9a,b,22] bromination–elimination cross-coupling protocol might also allow further tuning of the switching properties.

Experimental Section

General procedure

All reactions except for the Knoevenagel condensations were done under an argon atmosphere. All handling of photochromic compounds was carried out in the dark. THF was distilled over a Na/benzophenone couple. Thin-layer chromatography (TLC) was carried out on commercially available precoated plates (silica 60) with a fluorescence indicator. All melting points are uncorrected. UV/Vis absorption spectroscopy measurements were performed using a 1 cm-path-length cuvette. For compound **3**, UV/Vis absorption spectra were obtained by scanning the wavelength from 800 to 200 nm in a 1 cm-path-length cuvette using a Cary 50 Bio UV-visible spectrophotometer. Photoswitching experiments were performed on non-deoxygenated solutions using a 150 W xenon arc lamp equipped with a monochromator. The thermal back-reaction was performed by heating the sample (cuvette) by a peltier unit in the UV/Vis spectrophotometer. For compound **2**, UV/Vis absorption spectroscopy measurements were performed in a 1 cm-path-length cuvette using a Perkin–Elmer Lambda 1050 UV/Vis-NIR spectrometer. UV/Vis absorption spectra were obtained by scanning the wavelength from 600 to 200 nm for solutions in CH_3CN and C_6H_{12}, and from 600 to 290 nm for solutions in toluene. Photoswitching experiments were performed by using a homemade setup, which included four black-light lamps (F4WT5, Sylvania) with a UV radiation center at 368 nm (more details in the Supporting Information). NMR spectra were acquired using 500 MHz instruments equipped with a (non-inverse) cryoprobe or with a pentaprobe. All chemical-shift values in ^1H and ^{13}C NMR spectra are referenced to the residual solvent peak ($CDCl_3$ $\delta_H = 7.26$ ppm, $\delta_C = 77.16$ ppm; CD_3CN $\delta_H = 1.96$ ppm, $\delta_C = 1.94$ ppm). Mass spectra were recorded by using either a Bruker Solarix ESI-MALDI-FT-ICR instrument equipped with a 7 T magnet (prior to the experiments, the instrument was calibrated using sodium trifluoroacetate (NaTFA) cluster ions) or a Bruker MicrOTOF-QII system with an ESI source.

2,2′-(1,4-Phenylene)bis(1,8a-dihydroazulene-1,1-dicarbonitrile) (2)

Method 1: Et_3N (0.67 mL, 4.8 mmol) was added slowly over the course of 2 h to a stirred suspension of **4** (621 mg, 2.40 mmol) and freshly mortared tropylium tetrafluoroborate (857 mg, 4.82 mmol) in CH_2Cl_2 (50 mL) at −78 °C, and the reaction mixture was allowed to slowly warm to RT overnight. The reaction mixture was concentrated under vacuum, and the resulting dark yellow solid (compound **5**) was dissolved in DCE (100 mL). Tritylium tetrafluoroborate (1.66 g, 5.03 mmol) was added to this solution, and it was then heated to reflux for 2 h. The now red/black reaction mixture was cooled to 0 °C, and toluene (100 mL) was added followed by Et_3N (0.67 mL, 4.80 mmol). The temperature was allowed to reach RT. The resulting strongly red reaction mixture (which contained **6**) was heated to reflux for 1 h (to convert **6** into **2**), after which it was concentrated under vacuum. Purification by dry column vacuum chromatography (silica 15–40 μm, 12.6 cm^2; 1) 0–90% $CHCl_3$/heptanes, 5% steps, 40 mL fractions; 2) 0–100% toluene/heptanes, 10% steps, then 0–30% CH_2Cl_2/toluene, 5% steps, 40 mL fractions; 3) 0–60% EtOAc/heptanes, 5% steps, then 60–100% EtOAc/heptanes, 10% steps, 40 mL fractions) gave **2** (356 mg, 0.819 mmol, 34%) as a bright yellow solid with minor impurities. An analytically pure sample was obtained by recrystallization from boiling CH_3CN as bright yellow, thin needles. TLC (CH_2Cl_2): $R_f = 0.73$ (bright yellow); TLC (50% EtOAc/toluene): $R_f = 0.32$ (bright yellow); ^1H NMR (500 MHz, $CDCl_3$) $\delta = 7.84$ (s, 4H), 7.26 (s, 4H), 6.98 (s, 2H), 6.60 (dd, $J = 11.3$, 6.3 Hz, 2H), 6.51 (dd, $J = 11.3$, 6.1 Hz, 2H), 6.41 (br d, $J = 6.3$ Hz, 2H), 6.33 (ddd, $J = 10.2$, 6.1, 2.1 Hz, 2H), 5.84 (dd, $J = 10.2$, 3.8 Hz, 2H), 3.82 ppm (dt, $J = 3.8$, 2.1 Hz, 2H); ^{13}C NMR (125 MHz, $CDCl_3$) $\delta = 139.00$, 138.50, 133.68, 131.82, 131.59, 131.03, 127.93, 127.05, 122.13, 119.68, 115.06, 112.68, 51.23, 45.11 ppm (no splitting of signals with 0 Hz exponential apodization) (signals for diastereoisomers overlapping); HRMS (MALDI+, dithranol): *m/z* calcd for $C_{30}H_{18}N_4^{\bullet+}$: 434.15260; found: 434.15263 [$M^{\bullet+}$]; elemental analysis calcd (%) for $C_{30}H_{18}N_4$ (434.50): C 82.93, H 4.18, N 12.89; found: C 83.04, H 3.84, N 12.96.

Method 2: LiHMDS (2.6 mL, 1 M in toluene, 2.57 mmol) was added dropwise at −78 °C to a solution of **4** (302 mg, 1.17 mmol) in THF (50 mL). After 10 min, tropylium tetrafluoroborate (504 mg, 2.80 mmol) was added, and the reaction mixture was allowed to warm to RT over 2 h. Then the reaction mixture was quenched with saturated aqueous NH_4Cl (20 mL) and diluted with water (80 mL). It was extracted with diethyl ether (2×100 mL), dried with $MgSO_4$, and the solvent was removed under vacuum. The residue that contained **5** was dissolved in DCE (75 mL) and degassed with argon; then tritylium tetrafluoroborate (853 mg, 2.58 mmol) was added, and the mixture was heated to reflux for 2 h. The mixture was diluted with toluene and cooled to 0 °C, and Et_3N (0.36 mL, 2.58 mmol) was added dropwise to generate **6**. The reaction mixture was protected from light and left to stir while reaching RT. After 16 h, the reaction mixture was quenched with aqueous NH_4Cl (20 mL), then diluted with water (80 mL), extracted with diethyl ether (2×100 mL), dried with $MgSO_4$, and concentrated under vacuum. The remains were then purified by flash chromatography (20% CH_2Cl_2, 80% toluene to 100% CH_2Cl_2) to give **2** (440 mg, 87%) with a minor impurity, which could be removed by recrystallization from boiling CH_3CN to give compound **2** (105 mg, 21%).

2,2′-(1,3-Phenylene)bis(1,8a-dihydroazulene-1,1-dicarbonitrile) (3)

Et_3N (0.866 mL, 6.210 mmol) was added to a stirred suspension of **9** (801.9 mg, 3.105 mmol) and freshly mortared tropylium tetrafluoroborate (1.436 g, 8.072 mmol) in CH_2Cl_2 (175 mL) at −78 °C. The reaction mixture was allowed to slowly warm to RT overnight and then concentrated under vacuum. The resulting dark yellow solid (compound **10**) was dissolved in DCE (175 mL). Tritylium tetrafluoroborate (2.153 g, 6.521 mmol) was added to this solution, whereafter the mixture was heated to reflux for 1 h. The now red/black reaction mixture was cooled to 0 °C and toluene (175 mL)

was added, followed by Et_3N (0.866 mL, 0.210 mmol). The temperature was allowed to reach RT. The resulting strongly red reaction mixture (which contained **11**) was heated to reflux for 1 h to convert **11** into **3**, whereafter it was concentrated under vacuum. Purification by dry column vacuum chromatography (silica 15–40 μm, 12.6 cm^2, 0–100% $CHCl_3$/heptanes, 5% steps, 40 mL fractions) gave **3** (1.24 g) as a yellow solid with some impurities. An analytically pure sample was obtained by recrystallization from boiling $CHCl_3$ (50 mL) and 96% EtOH (100 mL), which gave **3** (498 mg, 40%) as a bright yellow crystalline powder. TLC (CH_2Cl_2): $R_f = 0.73$ (yellow to orange-red). M.p. $>230\,^\circ C$, darkens at 215–218 °C; ^1H NMR (500 MHz, $CDCl_3$): $\delta = 8.04$ (t, $J = 1.9$ Hz, 1H), 7.80 (dd, $J = 7.9$, 1.9 Hz, 2H), 7.61 (t, $J = 7.9$ Hz, 1H), 6.97 (s, 2H), 6.60 (dd, $J = 11.2$, 6.2 Hz, 2H), 6.51 (dd, $J = 11.2$, 6.2 Hz, 2H), 6.42 (d, $J = 6.2$ Hz, 2H), 6.33 (ddd, $J = 10.2$, 6.1, 2.2 Hz, 2H), 5.83 (dd, $J = 10.2$, 3.8 Hz, 2H), 3.82 ppm (m, 2H) (the coupling constants are not paired as the spin systems could not be assigned); ^{13}C NMR (125 MHz, $CDCl_3$): $\delta = 139.01$, 139.00, 138.33, 138.31, 133.95, 131.82, 131.52, 131.03, 131.02, 130.43, 127.92, 127.49, 123.99, 122.09, 119.64, 119.62, 115.09, 115.07, 112.71, 112.69, 51.21, 45.38 ppm (signals missing due to overlap); HRMS (MALDI+): *m/z* calcd for $C_{30}H_{18}N_4Na^+$: 457.14237; found: 457.14262 [M+Na^+]; elemental analysis calcd (%) for $C_{30}H_{18}N_4$ (434.49): C 82.93, H 4.18, N 12.89; found: C 82.82, H 4.32, N 12.86.

2,2′-[1,4-Phenylenebis(ethan-1-yl-1-ylidene)]dimalononitrile (4)

1,1,1,3,3,3-Hexamethyldisilazane (3.29 mL, 15.8 mmol) was added to acetic acid (7.54 mL, 131 mmol) while keeping the temperature under 75 °C. 4-Acetylacetophenone (2.10 g, 13.0 mmol), malononitrile (1.71 g, 25.9 mmol), and acetic acid (3.76 mL, 65.7 mmol) were added to this mixture. The mixture was heated to 70 °C for 29 h, after which the reaction mixture was poured into water (100 mL). The precipitate was collected, washed with water (4×50 mL), and then quickly with 40% EtOH (40 mL), which gave **4** (3.28 g, 98%) as a white powder. M.p. 193–196 °C; ^1H NMR (500 MHz, $CDCl_3$): $\delta =$ 7.67 ppm (s, 4H), 2.66 ppm (s, 6H); ^{13}C NMR (126 MHz, $CDCl_3$): $\delta =$ 173.61, 139.15, 128.20, 112.31, 112.18, 86.64, 24.35 ppm; HRMS (ESP+): *m/z* calcd for $C_{16}H_{11}N_4Na^+$: 281.0798; found: 281.0744 [M+Na^+]; elemental analysis calcd (%) for $C_{16}H_{10}N_4$ (258.09): C 74.40, H 3.90, N 21.69; found: C 74.28, H 3.75, N 21.46.

2,2′-{1,4-Phenylenebis[2,2-di(cyclohepta-2,4,6-trien-1-yl)ethan-1-yl-1-ylidene]}dimalononitrile (7)

Et_3N (0.45 mL, 3.2 mmol) was added to a solution of **4** (165 mg, 0.638 mmol) and tropylium tetrafluoroborate (575 mg, 3.23 mmol) in CH_2Cl_2 (100 mL) at RT. After 2 h, four spots were observed on TLC, and more tropylium tetrafluoroborate (135 mg, 0.759 mmol) and Et_3N (0.12 mL, 0.86 mmol) were added. After a further 16 h, there was one main spot on TLC. The mixture was quenched with saturated aqueous NH_4Cl (50 mL) and washed with water, then dried with $MgSO_4$ and concentrated under vacuum. The residue was purified by flash chromatography (20% EtOAc, 80% heptane) and recrystallized from chloroform and heptane, which gave compound **7** (291 mg, 74%) as a yellow solid. A small amount was recrystallized from THF/heptane for X-ray crystallography. M.p. 171–172 °C; ^1H NMR (500 MHz, $CDCl_3$): $\delta = 7.21$ (s, 4H), 6.74–6.68 (m, 8H), 6.28–6.23 (m, 8H), 5.26 (dd, $J = 9.1$, 6.8 Hz, 4H), 4.87 (t, $J =$ 8,12 Hz, 4H), 3.76 (t, $J = 9.3$ Hz, 2H), 2.10 ppm (s, 4H); ^{13}C NMR (125 MHz, $CDCl_3$): $\delta = 180.20$, 131.59, 130.86, 128.40, 126.39, 125.97, 119.99, 118.16, 111.59, 111.55, 48.54, 40.54 ppm (two signals missing); HRMS (ESP+): *m/z* calcd for $C_{44}H_{34}N_4Na^+$: 641.2676; found: 641.2663 [M+Na^+]; elemental analysis calcd (%) for $C_{44}H_{34}N_4$: C 85.41, H 5.54, N 9.05; found C: 85.35, H 5.28, N 9.04.

2,2′-[(2*E*,2′*E*)-1,4-Phenylenebis(3-phenylallyl-1-ylidene)]dimalononitrile (8)

Tritylium tetrafluoroborate (142 mg, 0.430 mmol) was added to a dry and argon-degassed solution of compound **7** (103 mg, 0.166 mmol) in DCE (45 mL) under argon. The mixture was heated to reflux for 2 h and was then washed with brine (2×50 mL), dried with $MgSO_4$, and concentrated under vacuum. The residue was then purified by flash chromatography (20% EtOAc, 80% heptane) and recrystallized from CH_2Cl_2/heptane to give compound **8** (24 mg, 25%). ^1H NMR (500 MHz, $CDCl_3$): $\delta = 7.64$ (d, $J = 15.6$ Hz, 2H), 7.59 (s, 4H), 7.58–7.54 (m, 4H), 7.50–7.38 (m, 6H), 6.90 ppm (d, $J = 15.6$ Hz, 2H); ^{13}C NMR (126 MHz, $CDCl_3$) $\delta = 169.93$, 150.18, 135.94, 134.07, 132.32, 129.74, 129.47, 129.24, 124.03, 113.24, 112.44, 83.22 ppm; HRMS (MALDI+): *m/z* calcd for $C_{30}H_{18}N_4Na^+$: 457.14237; found 457.14255 [M+Na^+].

2,2′-[1,3-Phenylenebis(ethan-1-yl-1-ylidene)]dimalononitrile (9)

NH_4OAc (10.0 g, 130 mmol) and AcOH (30 mL, 500 mmol) were added to a stirred mixture of 1,3-diacetylbenzene (8.61 g, 53.3 mmol) and malononitrile (14.97 g, 226.6 mmol) in toluene. The flask was equipped with a Dean–Stark trap, and the reaction mixture was heated to reflux overnight. The reaction mixture was cooled for about 30 min, and while still hot it was poured into a mixture of brine (100 mL) and diethyl ether (100 mL) in a separation funnel. Diethyl ether (100 mL) was cautiously poured into the hot flask and the mixture was left at boiling for a few minutes to extract the product from the oil that formed in the flask and was transferred into the separation funnel. The ether phase was separated and washed with water (100 mL) and brine (100 mL), then dried with $MgSO_4$, filtered, and concentrated under vacuum. The resulting yellow residue was purified (in two separate batches) by means of dry column vacuum chromatography (silica 15–40 μm, 12.6 cm^2, 0–36% EtOAc/heptanes, 3% steps, 40 mL fractions), which gave **9** (9.91 g, 38.4 mmol, 72%) as a slightly yellow crystalline powder. Alternatively, the crude product could be purified by a fractional recrystallization from CH_2Cl_2/heptanes or boiling EtOH (150 mL) (Note 1), which gave **9** (6.73 g, 53%) as slightly yellow crystals. M.p. 151 °C (EtOH); ^1H NMR (500 MHz, $CDCl_3$): $\delta = 7.73$–7.65 (m, 4H), 2.68 ppm (s, 6H); ^{13}C NMR (125 MHz, $CDCl_3$): $\delta =$ 173.76, 136.99, 130.65, 130.39, 126.29, 112.44, 112.11, 86.73, 24.46 ppm; HRMS (MALDI+): *m/z* calcd for $C_{16}H_{10}N_4Na^+$: *m/z*: 281.07977; found: 281.07983 [M+Na^+]. Note 1: The residue was first attempted purified by recrystallization from boiling EtOAc/heptanes (1:5).

2,2′-{1,3-Phenylene-bis[2-(cyclohepta-2,4,6-trien-1-yl)ethan-1-yl-1-ylidene]}dimalononitrile (10)

Et_3N (0.866 mL, 6.210 mmol) was added to a stirred suspension of **9** (801.9 mg, 3.105 mmol) and freshly mortared tropylium tetrafluoroborate (1.436 g, 8.072 mmol) in CH_2Cl_2 (175 mL) at −78 °C, and the reaction mixture was allowed to slowly warm to RT overnight. Saturated aqueous NH_4Cl (50 mL) was added, and the organic phase was separated and concentrated under vacuum. Purification by means of dry column vacuum chromatography (silica 15–40 μm, 12.6 cm^2, 0–50% EtOAc/heptanes, 5% steps, 40 mL fractions) gave **10** (790 mg, 58%) as a yellow solid. The desired compound could also be isolated by fractional recrystallization from

CH_2Cl_2/heptanes, which gave **10** (504 mg, 37%) as dark yellow crystals from which some were suitable for X-ray crystallography. M.p. 197–199 °C (decomp); ^{1}H NMR (500 MHz, $CDCl_3$): $\delta = 7.63$ (app t, $J = 7.8$ Hz, 1H), 7.53 (dd, $J = 7.8$, 1.6 Hz, 2H), 7.41 (t, $J = 1.6$ Hz, 1H), 6.22 (app dt, $J = 9.3$, 3.2 Hz, 4H), 5.16 (app dd, $J = 9.3$, 6.8 Hz, 4H), 3.11 (d, $J = 8.0$ Hz, 4H), 2.20–2.13 ppm (m, 2H) (the coupling constants are not paired as spin systems could not be assigned); ^{13}C NMR (125 MHz, $CDCl_3$): $\delta = 176.27$, 135.95, 131.30, 130.45, 130.25, 127.05, 126.40, 122.65, 112.22, 111.87, 88.24, 38.27, 37.59 ppm (signals missing due to overlap); HRMS (MALDI+): *m/z* calcd for $C_{30}H_{22}N_4Na^+$: 461.17367; found: 461.17363 [M+Na^+]; elemental analysis calcd (%) for $C_{30}H_{22}N_4$: C 82.17, H 5.06, N 12.78; found: C 81.99, H 5.01, N 12.62.

CCDC-1015127 (**7**, red crystal), CCDC-1015128 (**7**, yellow crystal), CCDC-1015129 (**10**), CCDC-1015130 (DHA–DHA **3**), and CCDC-1016226 (DHA–DHA **2**) contain the supplementary crystallographic data for this paper. These data can be obtained free of charge from The Cambridge Crystallographic Data Centre via www.ccdc.cam.ac.uk/data_request/cif.

Acknowledgements

The University of Copenhagen is acknowledged for financial support as well as the Lundbeck Foundation, the Swedish Research Council (VR), the Danish Center for Scientific Computing, the Danish Research Council (FNU), and the Villum Foundation (for X-ray diffractometer).

Keywords: charge transfer · chromophores · conjugation · electrocyclic reactions · photochromism

[1] a) B. L. Feringa, *Acc. Chem. Res.* **2001**, *34*, 504–513; b) F. M. Raymo, M. Tomasulo, *Chem. Soc. Rev.* **2005**, *34*, 327–336; c) S. Saha, J. F. Stoddart, *Chem. Soc. Rev.* **2007**, *36*, 77–92; d) N. Weibel, S. Grunder, M. Mayor, *Org. Biomol. Chem.* **2007**, *5*, 2343–2353; e) K. Matsuda, H. Yamaguchi, T. Sakano, M. Ikeda, N. Tanifuji, M. Irie, *J. Phys. Chem. C* **2008**, *112*, 17005–17010; f) M. R. Banghart, A. Mourot, D. L. Fortin, J. Z. Yao, R. H. Kramer, D. Trauner, *Angew. Chem. Int. Ed.* **2009**, *48*, 9097–9101; *Angew. Chem.* **2009**, *121*, 9261–9265; g) X. Ma, H. Tian, *Chem. Soc. Rev.* **2010**, *39*, 70–80.

[2] a) H. Bouas-Laurent, H. Dürr, *Pure Appl. Chem.* **2001**, *73*, 639–665; b) H. Dürr, *General Introduction, in Photochromism: Molecules and Systems* (Eds.: H. Dürr, H. Bouas-Laurent), Elsevier, Amsterdam, **2003**, pp. 1–14.

[3] a) M. Irie, *Chem. Rev.* **2000**, *100*, 1685–1716; b) H. Tian, S. Yang, *Chem. Soc. Rev.* **2004**, *33*, 85–97; c) K. Matsuda, M. Irie, *J. Photochem. Photobiol. C* **2004**, *5*, 169–182; d) K. Szacilowski, *Chem. Rev.* **2008**, *108*, 3481–3548; e) M.-M. Russew, S. Hecht, *Adv. Mater.* **2010**, *22*, 3348–3360; f) A. A. Beharry, G. A. Wolley, *Chem. Soc. Rev.* **2011**, *40*, 4422–4437; g) H. M. Dhammika Bandara, S. C. Burdette, *Chem. Soc. Rev.* **2012**, *41*, 1809–1825; h) W. Szymański, J. M. Beierle, H. A. V. Kistemaker, W. A. Velema, B. L. Feringa, *Chem. Rev.* **2013**, *113*, 6114–6178; i) R. Göstl, A. Senf, S. Hecht, *Chem. Soc. Rev.* **2014**, *43*, 1982–1996.

[4] a) J. Daub, T. Knochel, A. Mannschreck, *Angew. Chem. Int. Ed. Engl.* **1984**, *23*, 960–961; *Angew. Chem.* **1984**, *96*, 980–981; b) T. Mrozek, A. Ajayaghosh, J. Daub in *Molecular Switches* (Ed.: B. L. Feringa), Wiley-VCH, Weinheim, Germany, **2001**, pp. 63–106; c) S. L. Broman, M. B. Nielsen, *Phys. Chem. Chem. Phys.* **2014**, *16*, 21172–21182.

[5] a) J. Daub, S. Gierisch, U. Klement, T. Knochel, G. Maas, U. Seitz, *Chem. Ber.* **1986**, *119*, 2631–2646; b) S Gierisch, J. Daub, *Chem. Ber.* **1989**, *122*, 69–75; c) H. Goerner, C. Fischer, S. Gierisch, J. Daub, *J. Phys. Chem.* **1993**, *97*, 4110–4117; d) J. Ern, M. Petermann, T. Mrozek, J. Daub, K. Kuldovà, C. Kryschi, *Chem. Phys.* **2000**, *259*, 331–337; e) S. L. Broman, S. L. Brand, C. R. Parker, M. Å. Petersen, C. G. Tortzen, A. Kadziola, K. Kilså, M. B. Nielsen, *Arkivoc* **2011**, 9, 51–67.

[6] a) S. Lara-Avila, A. V. Danilov, S. E. Kubatkin, S. L. Broman, C. R. Parker, M. B. Nielsen, *J. Phys. Chem. C* **2011**, *115*, 18372–18377; b) S. L. Broman, S. Lara-Avila, C. L. Thisted, A. D. Bond, S. Kubatkin, A. Danilov, M. B. Nielsen, *Adv. Funct. Mater.* **2012**, *22*, 4249–4258; c) T. Li, M. Jevric, J. R. Hauptmann, R. Hviid, Z. Wei, R. Wang, N. E. A. Reeler, E. Thyrhaug, S. Petersen, J. A. S. Meyer, N. Bovet, T. Vosch, J. Nygård, X. Qiu, W. Hu, Y. Liu, G. C. Solomon, H. G. Kjaergaard, T. Bjørnholm, M. B. Nielsen, B. W. Laursen, K. Nørgaard, *Adv. Mater.* **2013**, *25*, 4164–4170.

[7] M. Cacciarini, E. A. Della Pia, M. B. Nielsen, *Eur. J. Org. Chem.* **2012**, 6064–6069.

[8] a) T. J. Kucharski, Y. Tian, S. Akbulatov, R. Boulatov, *Energy Environ. Sci.* **2011**, *4*, 4449–4472; b) K. Moth-Poulsen, in *Organic Synthesis and Molecular Engineering* (Ed.: M. B. Nielsen), Wiley, Hoboken, USA, **2014**, pp. 179–196.

[9] a) S. L. Broman, M. Å. Petersen, C. G. Tortzen A. Kadziola, K. Kilså, M. B. Nielsen, *J. Am. Chem. Soc.* **2010**, *132*, 9165–9174; b) M. Å. Petersen, S. L. Broman, K. Kilså, A. Kadziola, M. B. Nielsen, *Eur. J. Org. Chem.* **2011**, 1033–1039; c) S. L. Broman, M. B. Nielsen, *Chem. Eur. J.* **2013**, *19*, 9542–9548.

[10] M. Santella, V. Mazzanti, M. Jevric, C. R. Parker, S. L. Broman, A. D. Bond, M. B. Nielsen, *J. Org. Chem.* **2012**, *77*, 8922–8932.

[11] J. Daub, J. Salbeck, T. Knöchel, C. Fisher, H. Kunkely, K. M. Rapp, *Angew. Chem. Int. Ed. Engl.* **1989**, *28*, 1494–1496.

[12] S. Kobatake, M. Irie, *Tetrahedron* **2003**, *59*, 8359–8364.

[13] a) T. Kaieda, S. Kobatake, H. Miyasaka, M. Murakami, N. Iwai, Y. Nagata, A. Itaya, M. Irie, *J. Am. Chem. Soc.* **2002**, *124*, 2015–2024; b) I. Jung, H. Choi, E. Kim, C. Lee, S. O. Kang, J. Ko, *Tetrahedron* **2005**, *61*, 12256–12263.

[14] a) T. Mrozek, H. Görner, J. Daub, *Chem. Commun.* **1999**, 1487–1488; b) T. Mrozek, *Neue photochrome Systeme basierend auf Zehn- und Sechselektronenumlagerungen*, Doctoral Dissertation, University of Regensburg, **2000**; c) T. Mrozek, H. Görner, J. Daub, *Chem. Eur. J.* **2001**, *7*, 1028–1040.

[15] L. Gobbi, P. Seiler, F. Diederich, *Helv. Chim. Acta* **2001**, *84*, 743–777.

[16] S. L. Broman, M. Jevric, A. D. Bond, M. B. Nielsen, *J. Org. Chem.* **2014**, *79*, 41–64.

[17] R. O. Loutfy, C. K. Hsiao, B. S. Ong, B. Keoshkerian, *Can. J. Chem.* **1984**, *62*, 1877–1885.

[18] S. L. Broman, A. U. Petersen, C. G. Tortzen, J. Vibenholt, A. D. Bond, M. B. Nielsen, *Org. Lett.* **2012**, *14*, 318–321.

[19] a) Y. Sugihara, J. Kanemaru, J. Saito, I. Murata, *Chem. Lett.* **1992**, 2393–2396; b) I. T. Badejo, R. Karaman, J. L. Fry, *J. Org. Chem.* **1989**, *54*, 4591–4596.

[20] Gaussian 09, Revision D.01, M. J. Frisch, G. W. Trucks, H. B. Schlegel, G. E. Scuseria, M. A. Robb, J. R. Cheeseman, G. Scalmani, V. Barone, B. Mennucci, G. A. Petersson, H. Nakatsuji, M. Caricato, X. Li, H. P. Hratchian, A. F. Izmaylov, J. Bloino, G. Zheng, J. L. Sonnenberg, M. Hada, M. Ehara, K. Toyota, R. Fukuda, J. Hasegawa, M. Ishida, T. Nakajima, Y. Honda, O. Kitao, H. Nakai, T. Vreven, J. A. Montgomery, Jr., J. E. Peralta, F. Ogliaro, M. Bearpark, J. J. Heyd, E. Brothers, K. N. Kudin, V. N. Staroverov, R. Kobayashi, J. Normand, K. Raghavachari, A. Rendell, J. C. Burant, S. S. Iyengar, J. Tomasi, M. Cossi, N. Rega, J. M. Millam, M. Klene, J. E. Knox, J. B. Cross, V. Bakken, C. Adamo, J. Jaramillo, R. Gomperts, R. E. Stratmann, O. Yazyev, A. J. Austin, R. Cammi, C. Pomelli, J. W. Ochterski, R. L. Martin, K. Morokuma, V. G. Zakrzewski, G. A. Voth, P. Salvador, J. J. Dannenberg, S. Dapprich, A. D. Daniels, Ö. Farkas, J. B. Foresman, J. V. Ortiz, J. Cioslowski, D. J. Fox, Gaussian, Inc., Wallingford CT, **2009**.

[21] TURBOMOLE V6.2 2010, a development of University of Karlsruhe and Forschungszentrum Karlsruhe GmbH, 1989–2007, TURBOMOLE GmbH, since 2007; available from http://www.turbomole.com.

[22] M. Cacciarini, S. L. Broman, M. B. Nielsen, *Arkivoc* **2014**, *1*, 249–263.

Received: September 29, 2014
Published online on January 14, 2015